Catalysis Today 142 (2009) 258–266

Contents lists available at ScienceDirect

Catalysis Today

journal homepage: www.elsevier.com/locate/cattod

The role of niobium in MCM-41 supported with Pt and Au—A comparative study of physicochemical and catalytic properties

Izabela Sobczak *

A. Mickiewicz University, Faculty of Chemistry, Grunwaldzka 6, 60-780 Poznan, Poland

ARTICLE INFO

Article history:
Available online 10 September 2008

Keywords:
Gold
Platinum
MCM-41
NbMCM-41
Characterization
FTIR co-adsorption of NO
C_3H_6
O_2
NO-SCR
Methanol oxidation
WGS process

ABSTRACT

This paper reviews a series of results, partly published recently, on niobosilicate mesoporous molecular sieves of MCM-41 type modified with noble metals (Pt, Au). Platinum is introduced to MCM-41 by impregnation technique, whereas gold is incorporated by two methods: during the synthesis by co-precipitation (COP) and by impregnation (IMP). Three fundamental features of the prepared materials have been considered: (i) texture/structure, (ii) noble metal state and dispersion, and (iii) catalytic activity. The latter has been tested in selective reduction of NO by propene, methanol oxidation and WGS process. The role of niobium, as well as the effect of the nature of noble metals and the preparation method on the physicochemical and catalytic properties of the final materials based on NbMCM-41 (in comparison with siliceous MCM-41) is demonstrated.

1. Introduction

In recent years, increasing attention has been paid to noble metal-supported catalysts because of their potential applications in industrially important chemical reactions and catalytic processes involved in environmental protection. Platinum and gold supported on various matrices are in the focus of this attention.

Platinum is a very popular metal in catalysis [1]. The history of platinum as catalyst begins in 1823, when Johann Wolfgang Dobereiner discovered the catalytic activity of platinum. His lighter based on the H_2 and Pt sponge became a huge commercial success. Since that time the application of platinum catalysts has grown continuously and nowadays it is a rapidly expanding commercially important field. Pt-containing catalysts are useful in petrochemical and general chemical plants and are becoming increasingly important as autocatalysts for pollution control.

Gold is an element that has fascinated people for millennia [2–4]. However, contrary to platinum, gold has been considered to be chemically inert and uninteresting for many years and it has long been believed to be inactive also in catalysis. The situation changed dramatically since the 1980s when Hutchings [5] and Haruta [6] reported that gold-catalysts exhibit high catalytic activity in acetylene hydrochlorination and low temperature CO oxidation. Since that time, it has been shown, that gold supported on various oxides exhibits a unique catalytic activity.

It is known that the catalytic activity of supported Pt and Au nanoparticles is remarkably sensitive to the nature of the matrix, as well as to the preparation method and pre-treatment conditions of the sample [2,3,7]. Recently, MCM-41 mesoporous molecular sieves have been used as supports for platinum [8–10] and gold [11,12]. MCM-41 materials exhibit a uniformly and hexagonally arranged mesopores, a very narrow pore size distribution in the mesoporous range (2–10 nm), high surface area (~1000 m^2/g) and large pore volumes (~1 cm^3/g) [13]. It has been found [11] that mesoporous MCM-41 support makes the high dispersion of metal nanoparticles, and the mesopores facilitate the transport of molecules. The framework of siliceous MCM-41 material can be modified by introduction of various transitions metals. Among them niobium silicalite MCM-41 was prepared in the group of Ziolek [14,15]. The incorporation of Nb(V) instead of Si(IV) in MCM-41 generates excess positive charge in the framework. It was proposed [16,17] that it was balanced by the charge of hydroxyl

---

* Tel.: +4861 8291305.
E-mail address: sobiza@amu.edu.pl.

0920-5861/$ – see front matter © 2008 Elsevier B.V. All rights reserved.
doi:10.1016/j.cattod.2008.07.027

groups. Dehydroxylation of NbMCM-41 leads to formation of active species according to the scheme:

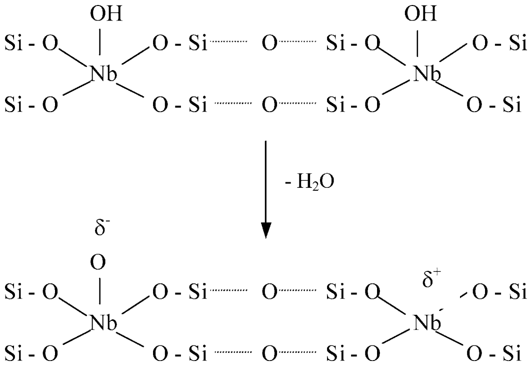

The presence of Nb–O$^{\delta-}$ and Nb$^{\delta+}$ species was designed on the basis of ESR, NO/FTIR studies [16] and the oxidative properties of NbMCM-41 in catalysis [17,18] which are due to the presence of active lattice oxygen formed during the dehydroxylation of molecular sieves. The generation of this active oxygen is accompanied by the formation of Lewis acid sites. Hexagonally ordered niobosilicate mesoporous materials denoted as NbMCM-41 make a new attractive support for Au and Pt. The presence of niobium in the MCM-41 matrix modified the physicochemical properties of the catalysts.

The aim of this work is to summarize the effect of niobium, the nature of noble metals and the preparation method on the physicochemical and catalytic properties of the final materials based on NbMCM-41 (in comparison with siliceous MCM-41). This paper reviews a series of results, partly published recently [19–25], on niobosilicate mesoporous molecular sieves modified with noble metals (Pt, Au). The catalytic applications of platinum and gold supported on NbMCM-41 matrix have been studied in several important processes: the reduction of NO$_x$ by hydrocarbons such as propene in the presence of oxygen excess, WGS process and methanol oxidation reaction.

2. Experimental

2.1. Catalyst synthesis and modification

MCM-41 mesoporous molecular sieves were synthesized by the hydrothermal method described in [13] and modified to prepare NbMCM-41 according to [14]. Si/Nb atom ratio was 128 as assumed.

Gold or platinum-containing catalysts were prepared via wetness impregnation of NbMCM-41 or MCM-41 with $HAuCl_4$ (Johnson Matthey, UK-USA) and H_2PtCl_6 (Aldrich), respectively, to obtain 1 wt.% of Au or Pt on the mesoporous support. Following the impregnation, the catalysts were dried at 373 K for 5 h and calcined at 773 K for 3 h in air. After calcination part of Pt-containing MCM-41 material was next reduced in H_2 (5 vol.% H_2/N_2) at 773 K for 3 h.

The alternative, direct synthesis of AuMCM-41 and AuNbMCM-41 (co-precipitation) was performed in the same manner as that of the conventional MCM-41 [13]. The only difference was the admission of $HAuCl_4$ and niobium oxalate (CBMM Brasil) as the sources of gold and niobium, respectively, into the gel containing sodium silicate and the template (CTACl – cetyltrimethylammonium chloride). The Si/Au atomic ratio was 256 (corresponding to 1 wt.% of Au).

2.2. Characterization

The prepared materials were characterized by XRD, nitrogen adsorption/desorption, UV–vis, the temperature-programmed reduction (H_2-TPR) and TOF-SIMS (*Time-of-flight secondary ion mass spectrometry*). These techniques were precisely described elsewhere [19–23].

2.3. FTIR spectroscopy

HC-SCR reaction was studied by in situ FTIR spectroscopy with $NO + C_3H_6 + O_2$ adsorption and co-adsorption, whereas catalytic properties of the materials in WGS process were characterized using an IR + MS Operando system. The details of the experiments were described in [19,22,23].

2.4. Methanol oxidation reaction

The methanol oxidation reaction was performed in a fixed-bed flow reactor. 0.02 g of the catalyst, with a size fraction of $0.5 < Ø < 1$ mm, was placed into the reactor. The samples were activated in helium flow (40 cm^3 min^{-1}) at 673 K for 2 h. The rate of heating was 15 K/min. After the activation, the temperature was decreased to that of the reaction. A portion of 40 ml/min He/O_2/MeOH (88/8/4 mol%) flow was used as a reactant mixture. The reactor effluent was analyzed using an online gas chromatograph (GC 8000 Top equipped with a capillary column of DB-1-FID detector and Porapak Q and 5A molecular sieves columns-TCD detector). Helium was applied as a carrier gas.

3. Catalysts and their characterization

The mesoporous molecular sieves of MCM-41 type described in this work are based on silicate framework, in which silicon is partially isomorphously substituted with niobium (Si/Nb = 128). The resulted NbMCM-41 was applied as a support for platinum or gold. The latter was also introduced by co-precipitation in one-pot synthesis. The catalysts studied in this work are listed in Table 1.

Table 1
Textural data of the catalysts (Pt-containing—after the reduction in H_2)

Catalyst	Surface area BET (m^2 g^{-1})	Mesopore volume BJH (cm^3 g^{-1})	Pore diameter BJH (nm)
MCM-41 (for Pt)	1073	0.99	3.9
Pt/MCM-41(IMP)	980	0.88	3.6
NbMCM-41 (for Pt)	961	0.83	3.6
Pt/NbMCM-41(IMP)	910	0.74	3.3
MCM-41 (for Au)	1076	1.25	3.9
Au/MCM-41(IMP)	1049	1.23	3.9
NbMCM-41 (for Au)	955	1.12	3.8
Au/NbMCM-41(IMP)	900	1.00	3.7
AuMCM-41 (COP)	886	0.81	2.9
AuNbMCM-41 (COP)	870	0.86	3.6

3.1. Texture/structure properties

All platinum or gold modified NbMCM-41 catalysts are hexagonally ordered mesoporous materials as shown by the X-ray diffraction and low temperature N_2 adsorption/desorption techniques. N_2 adsorption/desorption isotherms (shown in [19,21,23]) of Pt/NbMCM-41(IMP), Au/NbMCM-41(IMP) and AuNbMCM-41(COP) are of type IV according to the IUPAC classification. The texture parameters of these catalysts and those based on silicate support are given in Table 1. One can notice that all the structural parameters of the platinum or gold-catalysts depend on the nature of the matrix (silicate and niobosilicate) and the method of metal introduction [19,21,24]. The silicate MCM-41 exhibits the largest surface area, pore diameter and mesopore volume, whereas the introduction of niobium into the framework of MCM-41 causes a decrease in all these parameters. The presence of Pt or Au introduced by impregnation only slightly reduces the surface area and pore volume. In contrast, the introduction of gold during the synthesis of MCM-41 (co-precipitation) leads to the catalysts with smaller surface areas and pore volume relative to those in the impregnated materials [21,24].

XRD small-angle patterns of all impregnated platinum or gold MCM-41 samples studied (Fig. 1B) show the very typical hexagonal lattice verified by the observation of a strong single peak (1 0 0) centered at $2\Theta = 2^\circ$ and three peaks in the range of $2\Theta = 3^\circ–8^\circ$ [13]. The latter are due to the ordered hexagonal array of parallel mesoporous tubes and they are best resolved for the pristine MCM-41 supports (Fig. 1A). The similarities between XRD profiles of MCM-41 and NbMCM-41 and those of Pt/MCM-41(IMP), Pt/NbMCM-41(IMP) and Au/MCM-41(IMP), Au/NbMCM-41(IMP) demonstrate that the structure of MCM-41 materials is not destroyed either by the introduction of Pt or Au or by the following calcination (Au-samples) and reduction in H_2 (Pt-samples).

On the other hand, the introduction of gold during the synthesis leads to the catalysts with more disordered structure than that of the impregnated materials, irrespective of the nature of the matrix (Fig. 1B).

3.2. The state and surrounding of the noble metal

The state of platinum and gold in MCM-41 materials was studied by XRD, H_2-TPR and UV–vis techniques. The results clearly indicated the presence of metallic Pt and Au on the catalysts surface already after calcination [19–21,24,25]. In the wide-angle range of XRD patterns (Fig. 1C) the reflections characteristic of metallic platinum (at $2\Theta = 39.7^\circ$ and 46.2°) or metallic gold (at $2\Theta = 38.2^\circ$ and 44.8°) [8,26] are well visible. In the case of Pt-containing samples the peak at $2\Theta = 39.7^\circ$ originates from the (1 1 1) plane, whereas that at 46.2° from the (2 0 0) one. Both reflections are due to the cubic platinum metal structure [JCPDS-4-802] [26]. It is worthy of notice that, as shown in [19], for the catalyst containing niobium Pt/NbMCM-41(IMP) both peaks from metallic platinum are present in the XRD patterns after calcination, whereas for Pt/MCM-41(IMP), the peak at 46.2° appears after the reduction of the sample in H_2 [19]. It suggests that the temperature hydrogen treatment facilitates the reorganization of Pt clusters or causes the future reduction of Pt existing still in the PtO form on the pure silicate support. It is not the case for NbMCM-41 supporting platinum. Contrary, in the case of gold-MCM-41 both reflections from the Au-metal crystallites (Au(1 1 1) and Au(2 0 0)) were found in the XRD pattern of the calcined materials, irrespectively of the nature of the matrix and the method of gold introduction. It indicates that gold on the MCM-41 matrix is reduced much easier than platinum and that for gold MCM-41 samples the further treatment in H_2 is not necessary for reduction. The presence of metallic gold was confirmed by the UV–vis technique, the bands about 500 nm were observed in the spectra of all Au-samples studied (see [21,24]).

The important difference between calcined Pt and Au-MCM-41 materials is in the amount of the metal reduced. In contrast to Au/NbMCM-41(IMP), in the Pt/NbMCM-41(IMP) sample not only metallic but also cationic forms of noble metal were identified. The H_2-TPR profiles of Pt/NbMCM-41(IMP) shown in [19] include a low temperature (~390 K) peak assigned to the reduction of Pt^{2+} cations. It confirms a more difficult reduction of platinum than gold during calcination of noble metal-MCM-41.

The noble metal surrounding was studied by TOF-SIMS measurements and described in [20]. The results clearly indicate the presence of Pt in the surrounding of the oxygen atoms (leading to $Pt–O^-$ and/or $Pt–O_2^-$ ions, Table 2) [20]. The calculation of PtO^-/Pt, PtO_2^-/Pt^-, and PtO_2^-/PtO^- intensity ratios shows that for Pt/NbMCM-41 the PtO^-/Pt^- and PtO_2^-/Pt^- values are higher, whereas the PtO_2^-/PtO^- ratio is lower than that for Pt/MCM-41(IMP). It reveals that Pt on NbMCM-41 matrix has a higher number of oxygen atoms in the surrounding than Pt on MCM-41. The presence of niobium species in the catalysts system is responsible for an increase in the amount of oxygen in the surrounding of platinum and the presence of platinum decreases oxygen atoms number surrounding niobium species in the pristine support. This phenomenon can be interpreted by the interaction between Pt species and [Nb–O_x] leading to the transfer of oxygen from Nb to Pt. All Pt–O forms are significantly reduced during the hydrogen flow at 773 K, as evidenced by the decrease in PtO^-/Pt^- and PtO_2^-/Pt^- intensity ratios (Table 2). In contrast, for gold-catalysts, the ions

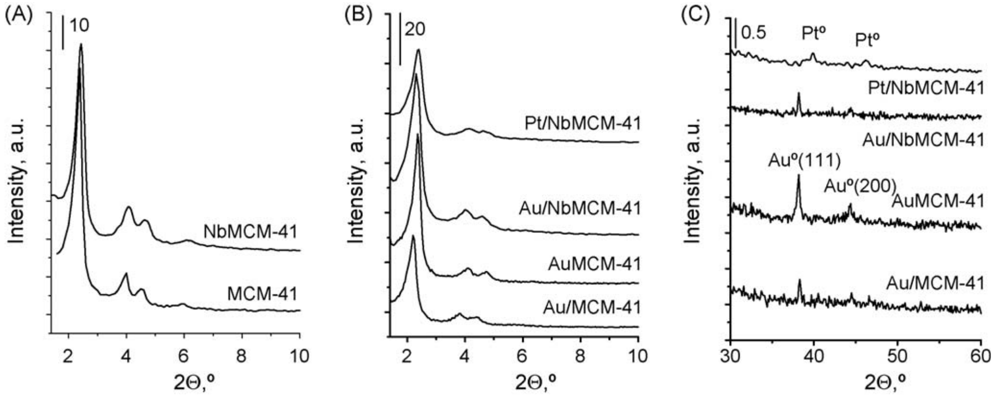

Fig. 1. XRD patterns of the catalysts: small-angle (A) (B) and wide-angle (C) XRD range.

Table 2
The TOF-SIMS intensity ratios of selected ions for Pt or Au-containing MCM-41 catalyst [20,21,24]

Catalysts	NbO^+/Nb^+	NbO_2^+/Nb^+	PtO^-/Pt^-	PtO_2^-/Pt^-	PtO_2^-/PtO^-	Cl^-/total	$PtCl^-/Pt^-$	$PtClO^-/Pt^-$	$AuCl^-/Au^-$	Au_3^-/Au^-
NbMCM-41	1.28	0.14	–	–	–	2.6×10^{-3}	–	–	–	–
Pt/NbMCM-41(IMP)	1.12	0.13	1.80	3.55	1.98	3.8×10^{-3}	0.95	0.55	–	–
Pt/NbMCM-41 (IMP) red. H_2	1.08	0.13	1.12	1.34	1.20	3.7×10^{-3}	0.73	0.75	–	–
Pt/MCM-41(IMP)	–	–	1.43	3.11	2.28	2.6×10^{-3}	0.87	0.50	–	–
Pt/MCM-41 (IMP) red. H_2	–	–	0.98	1.08	1.10	2.2×10^{-3}	0.48	0.38	–	–
Au/NbMCM-41(IMP)	1.16	0.10	–	–	–	4.1×10^{-3}	–	–	No signal	0.23
Au/MCM-41 (IMP)	–	–	–	–	–	1.9×10^{-3}	–	–	No signal	0.30
AuNbMCM-41(COP)	1.26	0.11	–	–	–	8.9×10^{-3}	–	–	No signal	0.15
AuNbMCM-41 (COP) as made (with template)	0.74	0.04			–	95×10^{-3}	–	–	0.16	0.10
AuMCM-41 (COP)	–	–	–	–	–	15×10^{-3}	–	–	1.46	0.12
AuMCM-41 (COP) as made (with template)	–	–	–		–	61×10^{-3}	–	–	0.19	0.11

indicating the Au–O bonding were not emitted in the TOF-SIMS study. This confirms the presence of only metallic gold on the surface of MCM-41 and NbMCM-41 [21,24].

A very important observation from the TOF-SIMS measurements was the identification of chlorine ions in the surrounding of both, gold and platinum centres in the calcined mesoporous catalysts [20,21]. However, whereas $PtCl^-$ were detected in the samples prepared by the impregnation, $AuCl^-$ ions were found only for the catalysts obtained by co-precipitation (as made materials still containing the surfactant (template)). Interestingly, the $AuCl^-/Au^-$ intensity ratio, which gives information on the amount of gold bonded to or surrounded by chloride ions, clearly increases for AuMCM-41(COP) and decreases to zero for AuNbMCM-41 after calcination. It means that the calcination of AuMCM-41(COP) causes the formation of the Au–Cl bond. The additional DTA/DTG experiment performed on AuMCM-41(COP) and described in [21] suggests that the difference in the residual chloride between the MCM-41 samples with Au introduced during the synthesis and by the post synthesis method is attributed to the interaction of Au-source with the template. The cationic surfactant (cetyltrimethylammonium cations) interacts with a part of $[AuCl_4]^-$ ions from $HAuCl_4$ and stabilizes the Au–Cl species. During calcination the surfactant is eliminated while the Au–Cl species become incorporated into the walls of the MCM-41 material. It has been evidenced [21] that the presence of the Au–Cl species is responsible for a very high basicity of AuMCM-41(COP). The presence of niobium in the framework of MCM-41 weakens the interactions of the surfactant with the $[AuCl_4]^-$ ions thanks to the strong Au–Nb interactions. That is why the chlorine ions are not localized in the surrounding of gold in AuNbMCM-41(COP) catalyst. On the other hand, the calculation of the $PtCl^-/Pt^-$ and $PtClO^-/Pt^-$ intensity ratios indicates that the reduction of Pt/MCM-41(IMP) catalyst in the flow of hydrogen at 773 K leads to the decrease in the values of intensity of the ions containing Cl and Pt. It shows that the reduction process removes Cl atoms from the surface more effectively than the calcination of Pt/MCM-41 sample. Moreover, contrary to Pt/MCM-41(IMP) material, in the case of Pt/NbMCM-41(IMP) the total Cl content is not influenced by the reduction treatment (Table 2). It suggests that Cl species are stronger held in the mesoporous niobosilicate than in the silicate matrix impregnated with Pt species. The same is true for Au-impregnated and calcined MCM-41 type materials.

3.3. The size and dispersion of noble metal

It is well known [2,3,27] that the catalyst activity depends on the size and dispersion of the metal supported on the matrix. The effect of the chemical nature of MCM-41 support and the treatment of the catalyst on the size and dispersion of platinum and gold present on the mesoporous MCM-41 matrix was studied by the TEM and TOF-SIMS methods and reported in [19–21]. It was found from the TEM results [19] that the presence of niobium in MCM-41 affected the properties of Pt-species. In Pt/MCM-41(IMP) the very high growth of the cluster size (from 6 to 20 nm) results from the reduction of the catalyst. Moreover, the thermal treatment in H_2 flow leads to interaction between Pt and Si and the platinum silicide (among others cubic Pt_3Si) particles are formed (particle size ~60 nm). Contrary, the particle sizes of Pt^0 dispersed on NbMCM-41 are less affected by the hydrogen reduction of the calcined material. The interaction of Pt with Nb species prevents Pt migration during heating. Thanks to that, the particle size of Pt does not increase significantly (from ca. 15 nm to ca. 17 nm for Pt/NbMCM-41(IMP)) and the dispersion of Pt after the reduction is higher than that on the MCM-41 matrix.

The determination of Pt dispersion on the surface of MCM-41 material was possible on the basis of the TOF-SIMS images [20]. The Pt/MCM-41(IMP) sample after calcination and reduction exhibits non-homogenous distribution of platinum, and only some platinum clusters are visible in the images (Fig. 2). The catalysts containing Nb in the matrix behave differently. The calcined and reduced Pt/NbMCM-41(IMP) reveals a good dispersion of Pt. Although the platinum signal is weak because of high ionization

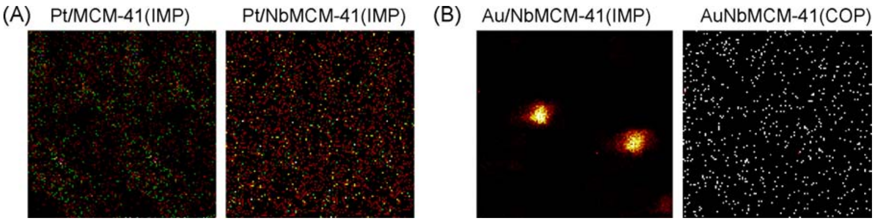

Fig. 2. TOF-SIMS images (200 μm × 200 μm) of Pt/MCM-41 (IMP); Pt/NbMCM-41(IMP) (A) and Au/NbMCM-41(IMP); AuNbMCM-41(COP) (B) catalysts. Bright color indicates Pt or Au ions.

energy of this metal, Pt seems to be distributed uniformly on the support surface. It indicates that Nb species in MCM-41 matrix prevent Pt migration and agglomeration during the calcination. That is why Pt dispersion is higher than that on the MCM-41 support.

Interestingly, it was found, that for gold-MCM-41 catalysts the size and dispersion of Au crystallites was determined not by the nature (chemical composition) of the matrix but mainly by the method of Au introduction. The size of Au crystallites in AuMCM-41(COP) was estimated as between 3 and 18 nm on the basis of the TEM images [21]. Gold particles on the TEM images of Au/MCM-41(IMP) have diverse dimensions and shapes (especially in the agglomerates) which makes it difficult to estimate their sizes. However, the peaks assigned to the metallic gold in the wide-angle XRD patterns (Fig. 1C) are sharper for the impregnated material suggesting larger Au agglomerates in the impregnated sample. Moreover, this feature was confirmed by the intensity ratio of Au_3^-/Au^- (TOF-SIMS) higher for Au/NbMCM-41(IMP) and Au/MCM-41(IMP) than for AuNbMCM-41(COP) and AuMCM-41(COP). The TOF-SIMS images allowed the estimation of Au dispersion on the surface of MCM-41 catalysts. Individual large Au clusters are visible on the surface of the impregnated catalyst (Fig. 2). In contrast, the TOF-SIMS images of AuNbMCM-41(COP) and AuMCM-41(COP) show a homogenous distribution of gold.

4. Processes

The mesoporous molecular sieves of MCM-41 type containing niobium in the framework (NbMCM-41) and their modified forms have been studied in various catalytic reactions [16–18,28–31] like: SCR process, catalytic decomposition of NO, synthesis of methanothiol, the oxidation reactions (e.g., oxidation of thioethers, cyclohexene, alcohols). Recently, of considerable interest have been the oxidizing properties of Nb-containing materials [16–18,29,30]. In the next sections the effect of Nb on the catalytic activity of bifunctional Pt–Nb and Au–Nb systems in the reduction of NO_x by propene in the presence of oxygen excess, in the WGS process and the oxidation of methanol will be discussed.

4.1. Selective catalytic NO reduction by propene

In the 1990s, Held et al. [32] and Iwamoto et al. [33,34] demonstrated the potential of using hydrocarbons in exhaust gases to selectively reduce nitrogen oxides even in the presence of a very large excess of oxygen (HC-SCR). Among a large number of zeolite, metal oxide and noble metal catalytic systems the Pt-(Pt/MFI, Pt/Al_2O_3, Pt/SiO_2) and Au-(Au/ZnO, Au/TiO_2, Au/Al_2O_3) catalysts have been reported to be active in this reaction [7,35–39].

Au or Pt containing NbMCM-41 catalysts characterized in this work have been studied by FTIR technique, the results are reported in [19,23]. The FTIR study of NO, C_3H_6 and O_2 adsorption and interaction allowed estimation of the possible chemisorption of the reagents and their interactions towards intermediates. It was found that NO adsorbed on metallic platinum present on the surface of Pt/NbMCM-41(IMP) (calcined and further reduced in H_2) and formed Pt^0-complex (1730 cm^{-1}) [9,10,40]. Moreover, NO adsorption leads to the creation of nitrate (NO_3^-) species characterized by an IR band 1630 cm^{-1}. It was indicated elsewhere [16,17] that this species was formed at $NbO^{\delta-}$ centres (identified in [16,17]) generated after dehydroxylation of Nb-containing MCM-41 materials. The formation of nitrates requires the oxidation of NO to NO_2. The latter is chemisorbed on NbO^- building NO_3^- species. Oxidation of NO is accompanied by its reduction to N_2O ($3NO \rightarrow N_2O + NO_2$). N_2O was observed in the gas phase. The introduction of gas oxygen causes the appearance of the intense band at ca. 1440 cm^{-1} which originates from nitrite (NO_2^-) species resulting from the NO oxidation to NO_2 [40] (Fig. 3) and electron transfer from the solid to NO_2 molecule. The same features were not detected for MCM-41 and Pt/MCM-41(IMP) samples, so this phenomenon has to be assigned to the properties of NbMCM-41 material used as a support for Pt.

Contrary, in Au/NbMCM-41(IMP) and AuNbMCM-41(COP), NO is not chemisorbed at the gold metallic centres [23]. Again, NO interaction with oxygen leads to formation of NO_2^- species (ca. 1400 cm^{-1}) (Fig. 3). Moreover, the chemisorbed NO_2 is observed in the FTIR spectra at ca. 1620 cm^{-1}. Thus, the presence of Nb in the matrix enhances the oxidation of NO towards NO_2 in comparison with that of Au/MCM-41(IMP).

The introduction of propene after the adsorption of NO followed by O_2 admission on both Pt/NbMCM-41(IMP) and Au/NbMCM-41(IMP) leads to partial oxidation of propene towards carboxylate species (the band at 1572 cm^{-1}, νCOO^- in acetate) [9,41,42] which transform to carbonates (1534 cm^{-1}) [43,44] at 523 K and acetone ($\nu C{=}O$ at 1727 cm^{-1}) and CO and CO_2 at 623 K (Fig. 3). Carboxylate and carbonate species are less stable on Au/NbMCM-41(IMP) and Pt/NbMCM-41(IMP) than on Pt/MCM-41(IMP) and Au/MCM-41(IMP) due to the Au–Nb or Pt–Nb interaction which weakens the chemisorption of intermediates. The weaker intermediates

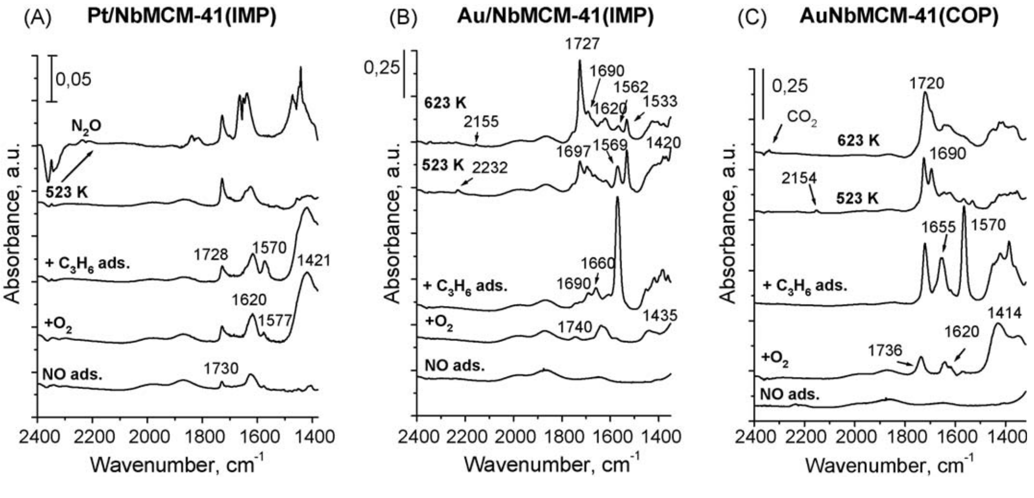

Fig. 3. FTIR spectra of Pt/NbMCM-41(IMP) (A), Au/NbMCM-41(IMP) (B) and AuNbMCM-41(COP) (C) materials after the admission of reagents at RT in the following order: NO, O_2, heating at 523 K, C_3H_6 introduction and heating at 523 and 623 K.

Table 3
Catalytic activity in MeOH + O_2 reaction (stationary state—average values)

Catalyst	Temp. (K)	MeOH conv. (%)	Selectivity (%)				
			HCHO	$HCOOCH_3$	CH_3OCH_3	$(CH_3O)_2CH_2$	CO_2
MCM-41	523	4	55	–	6	4	35
NbMCM-41	523	6	45	–	9	–	46
Au/MCM-41(IMP)	523	6	58	8	2	3	29
Au/NbMCM-41(IMP)	523	20	15	77	–	Traces	8
AuMCM-41(COP)	473	37	2	91		Traces	7
AuMCM-41(COP)	523	50	10	70	–	Traces	20
AuNbMCM-41(COP)	473	39	1	88	–	Traces	11
AuNbMCM-41(COP)	523	53	6	50	–	Traces	44

chemisorption leads to a more effective interaction with the adsorbed NO species manifested as the appearance of the band at 2150 cm^{-1} (chemisorbed CO) [45,46], adsorbed N_2O (2230 cm^{-1}) [40,43] and CO_2 (~2300 cm^{-1}) [46] formation after heating at 523 and 623 K. However, it is worth noting that the mechanism of HC-SCR-NO on Pt/NbMCM-41(IMP) and Au/NbMCM-41(IMP) is different. According to the FTIR data, the nitrate species (NO_2^-) formed after NO_2 chemisorption on Pt/NbMCM-41(IMP) are active in the interaction with propene towards total oxidation products via generation of acetate. In the Pt-catalyst, NbMCM-41 plays the role of storage of NO. In the oxidizing conditions NO is stored in the forms of nitrate and nitrite chemisorbed on Nb species. In the reduction step NO_2 is desorbed and interacts with propene.

Contrary to the behavior of Pt/NbMCM-41(IMP), in the Au-impregnated sample NO_2^- is formed but seems not to participate in the reaction with propene. On Au/NbMCM-41(IMP), NO is oxidized to NO_2, which reacts with chemisorbed propene towards carboxylates, further transformed to carbonates and acetone, and at higher temperatures to CO, CO_2, and N_2O. Because of a weaker interaction of Au–NbO_x than Pt–NbO_x, NO_2^- is stronger held on NbO_x species in Au/NbMCM-41(IMP) than in Pt/NbMCM-41(IMP). Thus, in Au/NbMCM-41(IMP) the support cannot play the storage role because NO_x is hardly released from that.

The effect of Nb on the activity of Pt/NbMCM-41(IMP) catalyst in the SCR-NO reaction and the storage properties of NbMCM-41 were also studied in transient conditions (in the flow of NO, O_2 and C_3H_6 – FTIR *Operando* system). The Operando experiments described in [25,47] confirmed that the presence of Nb in the support enhanced the activity of Pt-catalyst. Contrary to Pt/MCM-41(IMP), on Pt/NbMCM-41(IMP) propene was totally converted at 423–523 K. Moreover, the observed consumption of NO_2 after C_3H_6 admission indicates the role of NO_2 as the oxidation agent in the HC-SCR-NO process. On the other hand, the higher conversion of C_3H_6 on Pt/NbMCM-41(IMP) than on Pt/MCM-41(IMP) is supposed to favor hydrocarbon activation, enhancing its reduction properties. It was proposed [47] that the reaction pathway is based on the mechanism proposed by Burch et al. [48], in which Pt reduced particles are able to dissociate NO, the oxidized platinum is unable to break NO bond, while a high oxygen concentration on the catalytic surface leads to a selectivity towards N_2O more than N_2.

4.2. Methanol oxidation

Methanol is one of the most important chemical intermediates used in industrial chemistry. It is the starting reactant for the synthesis of various products, including hydrocarbons and mild oxidation products. The process of partial oxidation of methanol is nowadays intensively studied. Among the oxidation processes, formaldehyde production for the synthesis of phenolic resins is largely predominant [49]. Commercially, the selective oxidation of methanol to formaldehyde is carried out both on silver and ferric molybdate catalysts [49].

The results of methanol oxidation at 473 and 523 K (Table 3) clearly indicate that the introduction of Au by impregnation enhances the activity of MCM-41 and NbMCM-41 matrices. Moreover, Nb in the framework of NbMCM-41 increases the activity of impregnated MCM-41 and, what is important, significantly decreases the total oxidation towards CO_2 (from 29% for Au/MCM-41(IMP) to 8% for Au/NbMCM-41(IMP)). However, the Au/NbMCM-41(IMP) catalyst activates the reaction mainly towards methyl formate, whereas the main product formed on Au/MCM-41(IMP) is formaldehyde (58% selectivity) which is an important product because of industrial market demands.

The catalysts prepared by the co-precipitation method are much more active in methanol oxidation than those of the impregnated materials, but also less selective. The dramatic enhancement of the total oxidation to CO_2 is observed (20% for AuMCM-41(COP) and 44% for AuNbMCM-41(COP) at 523 K). Irrespectively of the chemical composition of the matrix, the main product of methanol oxidation on these catalysts is methyl formate. The basic character of AuMCM-41(COP) and AuNbMCM-41(COP) seems to be responsible for the high total oxidation of methanol to CO_2 that is enhanced by the presence of Nb besides gold. This behavior indicates that Au–Nb interaction in the skeleton makes the electron transfer much easier than in AuMCM-41 and therefore increases the CO_2 formation.

The FTIR experiments of MeOH adsorption described detail in [24] show that methanol is chemisorbed on all Au-catalysts in two forms: methoxy species manifested by the IR band at 1444 cm^{-1} and formate species giving rise to the band at ca. 1596 cm^{-1} (νCOO^-) [50,51]. According to the mechanism of methanol oxidation [49,51] this reaction requires the formation of chemisorbed methoxy groups, which are further transformed to formaldehyde species by the extraction of hydrogen with activated oxygen. If formaldehyde is chemisorbed strongly enough on the nucleophilic species it can interact with the next methanol molecule and form methyl formate. It was the case in the reaction performed on AuMCM-41(COP), and Au/NbMCM-41(IMP). The different effect of niobium on the selectivity of Au-containing samples depending on the preparation method has to be emphasized. When Au is introduced by impregnation the Au–NbO_x interaction is weaker than in one-pot synthesized sample and it makes the chemisorption of aldehyde species on gold centres stronger. This favors its further reaction towards formate. On the other hand, Nb–Au interaction in AuNbMCM-41(COP) weakens the chemisorption of aldehyde species decreasing the selectivity to methyl formate in comparison to AuMCM-41(COP). Simultaneously, the total oxidation of methanol to CO_2, which usually involves the radical mechanism, increases.

Contrary to gold-catalysts, Pt-containing samples were almost inactive towards partial oxidation products in methanol oxidation. A very high selectivity to CO_2 was observed already at 473 K (93% for Pt/NbMCM-41 and 85% for Pt/MCM-41).

4.3. WGS process

The water-gas shift (WGS) process ($CO + H_2O \rightleftarrows CO_2 + H_2$) is one of the important steps in the industrial production of hydrogen from hydrocarbons [52].

It is well known from the literature [53,54] that Pt-supported catalysts (mainly Pt/CeO_2) are one of the most active materials for WGS reactions at low temperatures. Generally, two mechanisms of the WGS process on Pt/CeO_2 are considered: (i) a redox process in which Pt is an active centre for CO chemisorption, leading to ceria reduction (via CO_2 production), which is then reoxidized in the interaction with H_2O, accompanied by hydrogen formation; (ii) a reaction of hydroxyl groups from reduced ceria with CO producing formate species, which decompose towards hydrogen. Moreover, it is known [55] that Nb added to the Pt-containing catalyst shifts the performance towards water-gas shift reaction over the competing methanation reaction.

However, it has been shown in last decade, that also gold-supported catalysts have high activity in the water-gas shift process at 398–448 K [2]. WGS reaction has been intensively studied on Au/CeO_2 and Au/CeO_2–ZrO_2 systems [2,56,57]. Different mechanisms of WGS process on these catalysts have been analyzed, in which Au^0 or $Au^{\delta+}$ are active species and oxygen comes from the support oxides or geminal hydroxyl groups. The latter are formed either by hydrogen spillover or by the reaction of water with the surface ion vacancies.

In order to study the activity of Pt-containing MCM-41 catalysts in the WGS process, Pt/NbMCM-41(IMP) and Pt/MCM-41(IMP) samples were first submitted to in situ IR analysis with CO adsorption [22]. FTIR spectra after CO adsorption on Pt/NbMCM-41 show the appearance of the band at 2060 cm^{-1} assigned to CO linearly coordinated on Pt small particles [58]. CO_2 and water were also formed, as shown by the bands at 2349 and 1636 cm^{-1}. Their production was firstly attributed to CO partial oxidation on Pt unreduced sites and to OH perturbation, respectively, as confirmed by the changes in the hydroxyl bands in the 3800–3300 cm^{-1} region. When Pt/NbMCM-41(IMP) was studied in the operando system under CO flow, mass spectra showed hydrogen production concomitantly with $CO \rightarrow CO_2$ oxidation and hydroxyl consumption when the temperature reached 473 K [22]. At 523 K, H_2 output was observed to be greater; it was maintained almost constant by water introduction in the stream. One can suppose that Nb–O species, which were found earlier [16] in NbMCM-41 sample, are the source of active oxygen and that they interact with CO forming CO_2. The following mechanism was proposed [22]:

$$Pt + CO \rightleftarrows Pt{-}CO$$

$$Pt - CO + 2{\equiv}SiOH \rightarrow CO_2 + H_2O + Pt + 2{\equiv}Si$$

$$Pt - CO + Nb{-}O \rightleftarrows Pt + Nb + CO_2$$

$$Nb + H_2O \rightleftarrows Nb{-}OH_2$$

$$NbOH_2 \rightleftarrows Nb{-}O + H_2$$

CO is chemisorbed on Pt species (the Pt–CO complex was detected in the IR spectra above 2000 cm^{-1}) and in this form it interacts with NbMCM-41 matrix leading to the abstraction of oxygen from Nb–O groups present on the surface. Nb in NbMCM-41 is coordinated to 4 oxygens in the skeleton and one on the surface [16]. The latter is mobile and easily interacts with CO chemisorbed on platinum species. This process leads to the formation of CO_2 and four coordinated $Nb^{\delta+}$ species. Water is chemisorbed on the latter species and finally hydrogen is formed when the Nb–O group is reconstituted.

The above observations indicate that the WGS phenomenon occurs on the Pt/NbMCM-41(IMP) catalyst. Interestingly, platinum catalysts based on silica MCM-41 without niobium species are not active in the reaction considered. There is no doubt that niobium promotes the WGS process.

Contrary, all gold-catalysts studied in this work (modified by impregnation: Au/MCM-41, Au/NbMCM-41 and co-precipitation: AuMCM-41) show low activity in the CO transformation to CO_2 under the CO and O_2 flow (400 ppm CO + 20 vol.% O_2 + Ar (gas vector) = 20 cm^3/min) [59] (Fig. 4). However, when the gold-catalysts were activated in the flow of CO (1 vol.% of CO + Ar = 25 cm^3/min) at 573 K, FTIR spectra show CO_2 formation during the activation. Similarly to Pt/NbMCM-41(IMP), this behavior is likely due to CO interaction with silanol OH groups, which are present on the surface of the MCM-41 matrix [16]. This process leads to the formation of CO_2 and H_2O:

$$CO + 2{\equiv}SiOH \rightarrow CO_2 + H_2O + 2{\equiv}Si \qquad (1)$$

Moreover, MS analysis showed hydrogen formation (Fig. 4B) as a result of the reaction between CO and H_2O:

$$CO + H_2O \rightarrow CO_2 + H_2 \qquad (2)$$

It indicates, that Au-containing MCM-41(COP) because of its highly basicity does not need niobium species for the activity in the $CO + H_2O$ reaction. It is worthy of notice, that when AuMCM-41(COP) were tested in an operando system under the $CO + H_2O$ flow at 573 K, it showed much higher H_2 production than Au/Al_2O_3

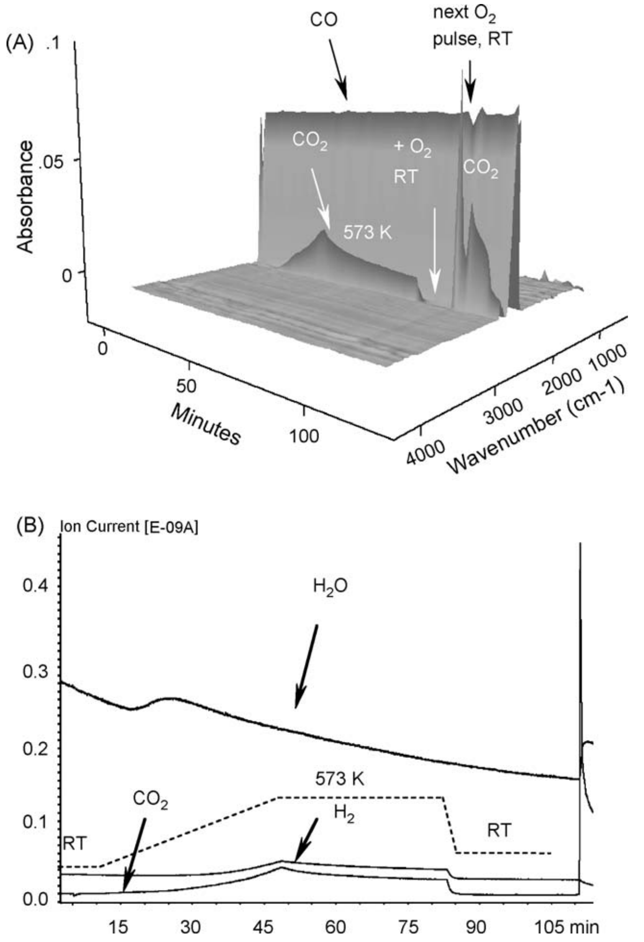

Fig. 4. FTIR spectra of gas phase (A) and MS profiles for masses 44 (CO_2), 2 (H_2), and 18 (H_2O) (B) on AuMCM-41(COP) sample under CO flow at 573 K.

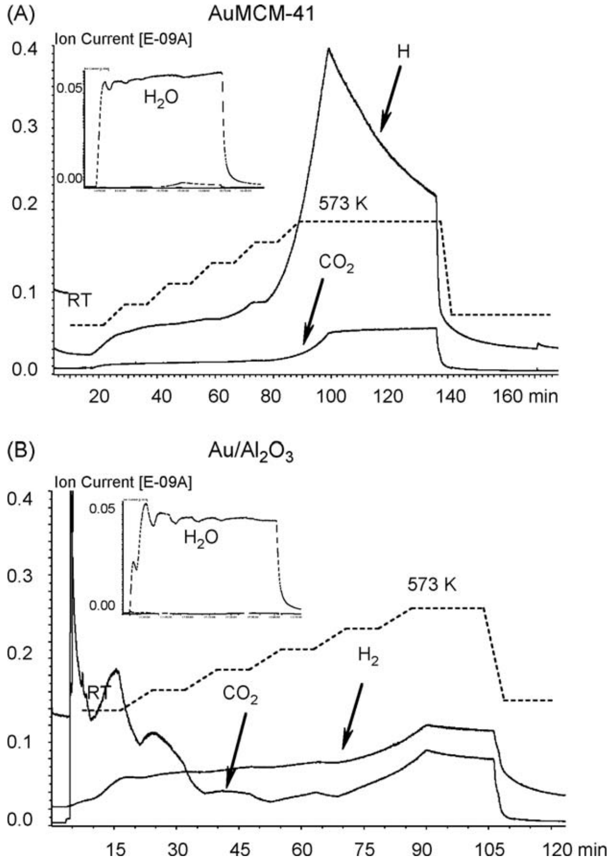

Fig. 5. MS profiles for masses 2 (H_2), 18 (H_2O) and 44 (CO_2) under CO and H_2O stream on AuMCM-41(COP) sample (A) and industrial Au/Al_2O_3 catalyst (B).

commercial catalyst with a very low concentration of hydroxyl groups on the surface (Fig. 5). The results obtained suggest that the proper support may provide centres for the WGS process and clearly indicate the important role of the siliceous MCM-41 matrix and OH groups.

In contrast to AuMCM-41 system, platinum-containing MCM-41 materials are active in the WGS reaction only when the NbMCM-41 support, containing active Nb–O_x species, is applied.

5. Conclusions

1. Platinum introduced by impregnation of MCM-41 samples is partly reduced during calcination, whereas gold is totally reduced under the same treatment.
2. [Nb–O_x] species in NbMCM-41 support contain mobile oxygen transferred to Pt loaded. Oxygen surrounded platinum species is significantly released after the reduction with hydrogen.
3. Gold species supported on NbMCM-41 are not surrounded by oxygen atoms.
4. The presence of chlorine in the platinum or gold modified MCM-41 has been evidenced and discussed. Chlorine atoms localized near Au in one-pot synthesized AuMCM-41 are responsible for the high basicity of the catalysts. The presence of niobium in NbMCM-41 support reduces the above-mentioned basicity because of a competition between Au–[NbO_x] and Au–Cl interactions.
5. The Pt–[NbO_x] interaction seems to be stronger than Au–[NbO_x] one because the former favors high platinum dispersion, whereas metallic gold dispersion is not influenced by the presence of niobium species in the NbMCM-41 matrix.
6. Gold dispersion is significantly determined by the method of Au introduction. The one-pot synthesis with Au-source leads to much better Au dispersion than the impregnation method irrespectively of the chemical composition of the mesoporous support.
7. The presence of $[NbO_x]^{\delta-}$ species in NbMCM-41 enhances the oxidation of NO to NO_2 in both Pt and Au loaded samples. Moreover, it weakens the chemisorption of the intermediates in HC-SCR-NO (because of Pt– and Au–NbO_x interaction) and enhances their interaction with nitrogen oxide species. However, as Pt–NbO_x interaction is stronger than Au–NbO_x one the nitrite species are more stabilized on the Au/NbMCM-41 than Pt/NbMCM-41 and less active in the interaction with partly oxidized propene. Therefore, Pt/NbMCM-41 system exhibits better storage properties in HC-SCR-NO than Au/NbMCM-41 one.
8. The gold-containing catalysts studied in this work exhibit much higher selectivity towards partial oxidation of methanol than the Pt-modified samples. The latter activate the total combustion of methanol to CO_2. Various strength of Au–NbO_x interaction depending on the preparation procedure (impregnation vs. co-precipitation) determines the product selectivity making formaldehyde production much higher when Au–NbO_x interaction is stronger.
9. Surface hydroxyls are involved in the WGS reaction on both, platinum and gold modified MCM-41 materials. However, Pt-containing materials are active in this reaction only when niobium species are located in the support.

Acknowledgements

I am grateful to Prof. Maria Ziolek from the Adam Mickiewicz University in Poznan, Poland, for very helpful discussion of the results.

I wish to thank Prof. Marco Daturi (ENSICaen and Université de Caen Basse-Normandie, Caen, France) and Dr. Jacek Grams (Technical University of Łódź, Poland) for their invaluable contribution in FTIR studies and TOF-SIMS measurements, respectively.

Polish Ministry of Research and Higher Education (grant 118/COS/2007/03) and COST D36/0006/06 are to be acknowledged for a partial support of this work.

Acknowledge is made also to Johnson Matthey (UK-USA) for supplying $HAuCl_4$.

References

[1] D. McDonald, L.B. Hunt, A History of Platinum and its Allied Metals, Johnson Matthey, London, 1982.
[2] G.C. Bond, C. Luis, D.T. Thompson, Catalysis by Gold, Imperial College Press, 2006.
[3] G.C. Bond, D.T. Thompson, Catal. Rev. -Sci. Eng. 41 (1999) 319.
[4] G.J. Hutchings, M. Haruta, Appl. Catal. A: Gen. 291 (2005) 2.
[5] G.J. Hutchings, D. Grady, Appl. Catal. 16 (1985) 441.
[6] M. Haruta, T. Kobayashi, H. Sano, N. Yamada, Chem. Lett. 2 (1987) 405.
[7] M. Haruta, Catal. Today 36 (1997) 153.
[8] S.-C. Shen, S. Kawi, Appl. Catal. B 45 (2003) 63.
[9] S.-C. Shen, S. Kawi, J. Catal. 213 (2003) 241.
[10] W. Schießer, H. Vinek, A. Jentys, Appl. Catal. B 33 (2001) 263.
[11] A. Wang, J.-H. Liu, S.D. Lin, T.-S. Lin, Ch.-Y. Mou, J. Catal. 233 (2005) 186.
[12] D.B. Akolekar, S.K. Bhargava, J. Mol. Catal. A 236 (2005) 77.
[13] J.S. Beck, J.C. Vartuli, W.J. Roth, M.E. Leonowicz, D.T. Kresge, K.D. Schmitt, C.T.W. Chu, D.H. Olson, E.W. Sheppard, S.B. McCullen, J.B. Higgins, J.L. Schlenker, J. Am. Chem. Soc. 114 (1992) 10834.
[14] M. Ziolek, I. Nowak, Zeolites 18 (1997) 356.
[15] M. Ziolek, I. Nowak, J.C. Lavalley, Catal. Lett. 45 (1997) 259.
[16] M. Ziolek, I. Sobczak, I. Nowak, P. Decyk, A. Lewandowska, J. Kujawa, Microporous Mesoporous Mater. 35–36 (2000) 195.
[17] M. Ziolek, I. Sobczak, A. Lewandowska, I. Nowak, P. Decyk, M. Renn, B. Jankowska, Catal. Today 70 (2001) 169.
[18] M. Ziolek, Catal. Today 78 (2003) 47.
[19] I. Sobczak, M. Ziolek, M. Nowacka, Microporous Mesoporous Mater. 78 (2005) 103.

[20] I. Sobczak, J. Grams, M. Ziolek, Microporous Mesoporous Mater. 99 (2007) 345.
[21] I. Sobczak, A. Kusior, J. Grams, M. Ziolek, J. Catal. 245 (2007) 259.
[22] I. Sobczak, J. Goscianska, M. Ziolek, J. Grams, Ch. Verrier, P. Bazin, O. Marie, M. Daturi, Catal. Today 114 (2006) 281.
[23] I. Sobczak, A. Kusior, M. Ziolek, Catal. Today 137 (2008) 203.
[24] I. Sobczak, A. Kusior, J. Grams, M. Ziolek, Stud. Surf. Sci. Catal. 70 (2007) 1300.
[25] I. Sobczak, M. Ziolek, J. Goscianska, F. Romero Sarria, M. Daturi, J.M. Jablonski, Stud. Surf. Sci. Catal. 158 (2005) 1319.
[26] J. Perez-Ramirez, J.M. Garcia-Cortes, F. Kapteijn, G. Mul, J.A. Moulijn, C. Salinas-Martinez de Lecea, Appl. Catal. B 29 (2001) 285.
[27] D. Trong On, D. Desplantier-Giscard1, C. Danumah, S. Kaliaguine, Appl. Catal. A: Gen. 253 (2003) 545.
[28] M. Ziolek, I. Sobczak, I. Nowak, M. Daturi, J.C. Lavalley, Topics Catal. 11 (2000) 343.
[29] I. Sobczak, M. Ziolek, M. Renn, P. Decyk, I. Nowak, M. Daturi, J.C. Lavalley, Microporous Mesoporous Mater. 74 (2004) 23.
[30] B. Kilos, M. Aouine, I. Nowak, M. Ziolek, J.C. Volta, J. Catal. 224 (2004) 314.
[31] P. Decyk, M. Trejda, M. Ziolek, C. R. Chim. 8 (2005) 635.
[32] W. Held, A. Koenig, T. Richter, L. Puppe, SAE Paper 900946 (1990).
[33] M. Iwamoto, in: Proceedings of Meeting of Catalytic Technology for Removal of Nitrogen Monoxide, Tokyo, January, (1990), p. 17.
[34] M. Iwamoto, H. Yahiro, Y. Yu-u, S. Shundo, N. Mizuno, Shokubai 32 (1990) 430.
[35] A. Fritz, V. Pitchon, Appl. Catal. B: Environ. 13 (1997) 1.
[36] Y. Traa, B. Burger, J. Weitkamp, Microporous Mesoporous Mater. 30 (1999) 3.
[37] M.D. Amiridis, T. Zhang, R.J. Farrauto, Appl. Catal. B: Environ. 10 (1996) 203.
[38] L.Q. Nguyen, Ch. Salim, H. Hinode, Appl. Catal. A: Gen. 347 (2008) 94.
[39] A. Ueda, T. Oshima, M. Haruta, Appl. Catal. B: Environ. 12 (1997) 81.
[40] K. Hadjiivanov, Catal. Rev. -Sci. Eng. 42 (2000) 71.
[41] P. Sazama, L. Capek, H. Drobná, Z. Sobalík, J. Dedecek, K. Arve, B. Wichterlová, J. Catal. 232 (2005) 302.
[42] M. Haneda, N. Bion, M. Daturi, J. Saussey, J.-C. Lavalley, D. Duprez, H. Hamada, J. Catal. 206 (2002) 114.
[43] T.E. Hoost, K.A. Laframboise, K. Otto, Appl. Catal. B: Environ. 7 (1995) 79.
[44] E. Finocchio, G. Busca, V. Lorenzelli, R.J. Willey, J. Catal. 151 (1995) 204.
[45] A. Simakov, I. Tuzovskaya, A. Pestryakov, N. Bogdanchikova, V. Gurin, M. Avalos, M.H. Farıas, Appl. Catal. A: Gen. 331 (2007) 121.
[46] M. Manzoli, F. Boccuzzi, A. Chiorino, F. Vindigni, W. Deng, M. Flytzani-Stephanopoulos, J. Catal. 245 (2007) 308.
[47] J. Goscianska, P. Bazin, O. Marie, M. Daturi, I. Sobczak, M. Ziolek, Catal. Today. 119 (2007) 78.
[48] R. Burch, J.A. Sullivan, T.C. Watling, Catal. Today 42 (1998) 13.
[49] J.M. Tatibouet, Appl. Catal. A: Gen. 148 (1997) 213.
[50] G. Busca, A.S. Elmi, P. Forzatti, J. Phys. Chem. 91 (1987) 5263.
[51] G. Busca, J. Lamotte, J.-C. Lavalley, V. Lorenzelli, J. Am. Chem. Soc. 109 (1987) 5197.
[52] C.H. Bartolomew, R.J. Farrauto, in: C.H. Bartolomew, R.J. Farrauto (Eds.), Fundamentals of Industrial Catalytic Processes, Wiley, Hoboken, NJ, 2006, p. 909.
[53] G. Jacobs, U.M. Graham, E. Chenu, P.M. Patterson, A. Dozier, B.H. Davis, J. Catal. 229 (2005) 499.
[54] A. Goguet, F. Meunier, J.P. Breen, R. Burch, M.I. Petch, A. Faur Ghenciu, J. Catal. 226 (2004) 382.
[55] A. Hagemeyer, C.J. Brooks, R. Carhart, K. Yaccato, C.B. Phillips, P. Strasser, R.K. Grasselli, US2004177556 (2004).
[56] D. Andreeva, Gold Bull. 35 (2002) 82.
[57] T. Tabakova, F. Boccuzzi, M. Manzoli, D. Andreeva, Appl. Catal. A: Gen. 252 (2003) 385.
[58] P. Bazin, O. Saur, J.C. Lavalley, M. Daturi, G. Blanchard, Phys. Chem. Chem. Phys. 7 (2005) 187.
[59] W. Klimas, I. Sobczak, O. Marie, P. Bazin, M. Daturi, M. Ziolek, Polish J. Chem. 82 (2008) 1695.